Published in final edited form as:
Biochim Biophys Acta. 2012 August ; 1823(8): . doi:10.1016/j.bbamcr.2012.05.017.

Inhibitory role of adiponectin peptide I on rat choroidal neovascularization

Valeriy V. Lyzogubov, **Ruslana G. Tytarenko**, **Nalini S. Bora**, and **Puran S. Bora***
Department of Ophthalmology, Jones Eye Institute, Pat & Willard Walker Eye Research Center, 4301 West Markham, University of Arkansas for Medical Sciences, Little Rock, Arkansas, 72205.

Abstract

Age-related macular degeneration (AMD) is a leading cause of central blindness in elderly population. Wet type of AMD is characterized by extensive growth of new vessels. One of the effective strategies to treat wet AMD is to limit the choroidal neovascularization (CNV). We studied effect of adiponectin peptide I (APNpI) on new vessel growth in laser-induced rat model of wet AMD and on rat choroidal endothelial cell (CEC) culture. CNV size and vessel density was investigated by microscopy. Immunohistochemical staining (IHC) for Von Willebrand Factor (vWF), APN, APN receptors 1 (AdipoR1), 2 (AdipoR2), VEGF, VEGF receptor 2 (VEGF-R2), proliferating cell nuclear antigen (PCNA) was performed in CNV area. The mRNA expression of VEGF and VEGF-R2 in RPE-choroid was investigated by RT-PCR and real-time PCR. APNpI inhibited area of CNV by 4 fold, number of vWF positive vessels by 99% and area of subretinal tissue by 40%. The expression of VEGF and VEGF-R2 at mRNA and protein levels were decreased after APNpI treatment in vivo. Proliferative index (PCNA) was 5 fold less in laser spots of APNpI treated rats compared to controls. In conclusion, APNpI inhibited formation of new vessels in rat model of CNV by decreasing VEGF, VEGF-R2 expression and cell proliferation. Thus, APNpI may have potential therapeutic use for AMD treatment since it significantly inhibited CNV.

Keywords

Adiponectin; Adiponectin receptors; VEGF; Angiogenesis; Macular degeneration; Neovascularization; Proliferation

1. Introduction

Age-related macular degeneration (AMD) is a leading cause of blindness in elderly population [1–3]. Wet type of AMD is characterized by extensive growth of new vessels [2–5]. One of the effective strategies in treatment of AMD in humans is to limit choroidal neovascularization (CNV) by acting on VEGF related signaling pathway which is involved in pathogenesis of AMD [3–5]. Anti-VEGF drugs are successfully being used for inhibition of CNV [4]. However, these drugs have some serious side effects: endophthalmitis,

***Corresponding author:** Dr. Puran S. Bora, 4301 West Markham, Department of Ophthalmology, Jones Eye, Institute, Pat & Willard Walker Eye Research Center, University of Arkansas for Medical, Sciences, Little Rock, Arkansas, 72205. USA, tel. +1 501 686 8293, fax. +1 501 686 8316, pbora@uams.edu.

rhegmatogenous retinal detachment, retinal tear, uveitis, and vitreous hemorrhage [6]. Therefore development of new drugs which may be more effective and have fewer side effects is necessary as an alternative to current treatments. One of the possible candidates for treatment of AMD in humans may be adiponectin (APN) or peptides derived on the structural basis of the APN. APN is a plasma protein, secreted predominantly by adipose cells and mimics many metabolic actions of insulin [7, 8]. The expression of APN was shown in numerous tissues suggesting the importance of APN in regulation of local processes [8–10]. Additionally to its metabolic functions, APN acts as a regulator of angiogenesis and proliferation [11–19]. APN shares sequence homology with a family of proteins showing a modular design containing a C-terminal complement factor C1q-like globular domain and the C-terminal globular domain [20]. However, the mechanism by which APN acts is poorly understood. The aim of this study is to understand the role of APN peptide I on CNV in rats and to investigate the expression of VEGF, VEGF receptor 2 in the retinal pigment epithelium (RPE) and choroid. In the present study we have shown the role of APN peptide I in the regulation of VEGF and VEGF receptor 2 in rat eye. As an angiogenesis inhibitor, APN may also have therapeutic implications in the treatment of age related macular degeneration.

2. Methods

2.1. Animals

Male Brown Norway rats, 6–7 weeks old, from Harlan Sprague Dawley, Inc. were used. This study was approved by the Institutional Animal Care and Use Committee (IACUC), University of Arkansas for Medical Sciences (UAMS), Little Rock, AR.

2.2. Choroidal endothelial cells (CECs) culture and APNpI administration

CECs were isolated from eyes as described [21] with modifications. Brown Norway rats (n=3 rats) were sacrificed and eyes were removed under sterile conditions. Eyes were treated with 70°C ethanol for 30 seconds and washed with Dulbecco's phosphate buffered saline (DPBS, Mediatech, Manassas, VA) for 1 minute (3 times). Eyes were dissected and anterior part of the eyes, lens and retina was removed. RPE-choroid was separated from sclera by scrapping and transferred to DPBS. RPE-choroid tissue was treated with 0.25% Trypsin (HyClone, Logan, UT) for 30 minutes. RPE-choroid cells were incubated in selective medium MCDB-1 with fetal bovine serum and antibiotics (VEC technologies, Rensselaer, NY) in 25 sm^2 flasks under condition of 5% CO_2 and 37°C. After 2 passages cells were investigated for presence of endothelial cell markers CD31, von Willebrand Factor (vWF) and Isolectin IB4 (ILIB4). We used $CD31^+$ vWF^+ILIB4^+ endothelial cells, from 3^{rd} to 5^{th} passage (split ratio 1:3), 50 cells per 1 mm^2 of surface area.

Adiponectin peptide I (APNpI, NH2-KDKAVLFTYDQYQEKNVD-COOH, GenScript, and Piscataway, NJ) was dissolved in sterile deionized water. Concentration 80 μg/mL of APNpI was prepared using MCDB-1 medium. Treatment of CECs with APNpI was performed during 12 hours. All experiments were repeated 3 times.

2.3. Induction of CNV in rats and APN peptide I administration

Animals were divided into 3 groups. CNV was induced by Argon laser (Lumenis Inc., Santa Clara, CA) as previously described [22–26]. Three laser spots (spot size – 50 μm; duration - 0.05 s; power - 360 mW) were placed in each eye close to the optic nerve. Groups 1 (n=45 rats) and 2 (n=45 rats) were lasered and group 3 (n=20 rats) was not treated with laser and used as a control. We synthesized 5 peptides (each of 18 amino acids) from globular region of adiponectin, which has no homology with the complement component 1q (C1q). We tested all 5 peptides but found that 2 mg/animal/day of adiponectin peptide I (APNpI, NH2-

KDKAVLFTYDQYQEKNVD-COOH, Peptide Biochemical Research Inc., Seattle) has maximum effect in rats. APNpI was injected intraperitoneally (dose of 2 mg/animal/day) 1 day before laser treatment and then every day until animals were sacrificed. Group 1 received PBS, group 2 was injected with APNpI and group 3 was not injected.

2.4. CNV size evaluation

Size of CNV was determined as described before [22–26]. Briefly, 10 days after laser treatment, 5 animals from group 1 (PBS injected) and group 2 (APNpI injected) were anesthetized with ketamine and xylazine, perfused with 2 ml of PBS containing 50 mg/ml fluorescein isothiocyanate labeled dextran (average molecular mass 2,000,000; Sigma-Aldrich, St. Louis, MO) and sacrificed. Eyes were fixed in normal buffered formalin (Sigma-Aldrich, St. Louis, MO) for 4 hours. After dissection of the eyes, the RPE-choroid-sclera complexes were stained for elastin using antibody (Santa Cruz Biotechnology, CA) and flat mounted in water soluble Durcupan (Sigma-Aldrich, St. Louis, MO). Images of laser injured areas were captured using confocal microscope LSM510 (Carl Zeiss, Jena GmbH). The size of CNV was determined by morphometric analysis using the ImageJ program (National Institutes of Health, Bethesda, Maryland, USA). Areas of green (FITC-dextran perfused vessels or CNV) and red fluorescence (elastin positive) were measured and percentage of CNV area was calculated.

2.5. Histology

CNV was induced in rats and APNpI or PBS was injected as described. Eyes were fixed in 10 days after laser treatment in 10% formalin solution (Sigma-Aldrich, St. Louis, MO) for 24 hours, dehydrated in ethanol and embedded in paraffin. Four-micron serial sections were cut. After deparaffinization in xylene and hydration sections were stained with hematoxylin and eosin (Electron Microscopy Sciences, Hatfield, PA). Stained sections were dehydrated in ethanol, cleaned in xylene and mounted in Permount (Electron Microscopy Sciences, Hatfield, PA). After drying for at least 48 hours, sections were used for morphological analysis. Images of laser injured area of the choroid were captured using QImaging GO-5 camera (Surrey, BC, Canada) and Olympus microscope.

2.6. Immunohistochemistry and immunocytochemistry

We used above mentioned serial sections for immunohistochemical (IHC) studies and cultured CECs for immunocytochemical (ICC) investigations. Goat polyclonal anti-rat $VEGF_{164}$ antibody (R&D Systems, Minneapolis, MN), goat anti-adiponectin antibody (R&D Systems, Minneapolis, MN), rabbit polyclonal anti-VEGF receptor 2 antibody (Affinity Bioreagents, Golden, CO), rabbit anti-Von Willebrand Factor endothelial marker (Affinity Bioreagents, Golden, CO), goat polyclonal anti-PCNA antibody (Biovision, Mountain View, CA), rabbit anti-adiponectin receptor R1 and R2 serum (both from Phoenix, Pharmaceuticals, Belmont, CA), rabbit anti-adiponectin R1 antibody (Abcam, Cambridge, MA), goat anti-CD31 antibody (Santa Cruz, Santa Cruz, CA) were used as primary antibody. For double immunohistochemical staining we used secondary rabbit anti-goat IgG (H+L)-FITC, rabbit anti-goat IgG (H+L)-AF594, goat anti-rabbit IgG (H+L)-FITC and Isolectin IB4 AF594 conjugate purchased from Invitrogen (South San Francisco, CA). Sections were mounted in ProLong antifade reagent (Invitrogen, South San Francisco, CA). We also used secondary biotinylated anti-goat or anti-rabbit affinity purified IgG (H+L), Vectastain Elite ABC Kit with horse-radish peroxidase, Vector VIP substrate KIT for peroxidase which gives purple color of specific staining and Vector Methyl green nuclear counterstain (all fromVector Laboratories, Burlingame, Ca). For immunocytochemical study CECs were incubated in Lab-Tek chamber slide system (Nalge Nunc, Naperville, IL) in MCDB-1 complete medium for 24 hours in 5% CO_2 atmosphere and 37°C temperature. Cells were fixed in methanol for 20 minutes on ice, washed with DPBS and stained using

endothelial cell markers CD31, von Willebrand Factor (vWF) and Isolectin IB4 (ILIB4). Control stains were performed with isotype matched control antibodies at concentrations similar to those of the primary antibodies and staining by omission of the primary or secondary antibodies. Sections were mounted using Permount (Electron Microscopy Sciences, Hatfield, PA). Cells observation and capturing of sections was made using an Olympus microscope equipped with QImaging Go-5 camera (Surrey, BC, Canada).

2.7. Colocalization of adipoR1 receptors and APNpI

We investigated binding of APNpI to RPE-choroid tissue in vivo and to endothelial cells in vitro using method of double IHC or ICC. We used FITC labeled APNpI (APNpI-FITC, GenScript, and Piscataway, NJ). We dissolved APNpI-FITC in sterile deionized water and prepared 80 μg/mL solution of APNpI-FITC in DPBS. We induced CNV in rats as described above and injected 5 μL of APNpI-FITC or DPBS subretinal to naïve rats and laser treated animals at day 7 post-laser. We sacrificed animals in 1 hour after injection, harvested eyes and placed them in Tissue-Tek O.C.T compound (Sakura Finetek, Torrance, CA). The eyes were snap frozen using Frostbite (Surgipath Medical Industries, Richmond, IL) and stored at −80°C. Cryosections (20 μm) were cut and fixed with ice cold methanol for 20 minutes. Sections were additionally stained for adipoR1 by IHC. Rat CECs were incubated in Lab-Tek chamber slide system (Nalge Nunc, Naperville, IL) in MCDB-1 complete medium for 24 hours in 5% CO_2 atmosphere and 37°C temperature. Cells were fixed in methanol for 20 minutes on ice, washed with DPBS and treated with 80 μg/mL of APNpI-FITC for 1 hour at 37°C in humid chamber. Cells additionally were stained for adipoR1 by ICC. Sections and cells were mounted in ProLong antifade reagent with DAPI (Invitrogen, South San Francisco, CA). We used ZEISS LSM 510 laser confocal microscope set up with Beam Splitters as follows: 488 nm laser (25%) window 505–550 nm, 561 nm laser (25%) window 575–615 nm. Eight bit images were obtained using the microscope in sequential mode with line average of 16 and format 1024 × 1024 pixels and in one single plane (1 μm optical slice). We used Plan-Apochromat 63× / 1.4 objective and Immersol 518 F oil (ne = 1.518 (23°C) Carl Zeiss, Oberkochen, Germany).

2.8. Semiquantitative scoring of IHC staining

We investigated sections of naïve or laser treated rats at day 10 post laser injury (n=5 rats in each group and 15 spots in each group), that were stained for AdipoR1 and AdipoR2. Semiquantitative scoring of positive signal in choroidal vessels and RPE cells located in spot area was performed as described before [15]. The intensity of staining was graded from 0 to 3 (0 – no staining; 1 – faint; 2 – moderate; 3 – intense).

2.9. Vessel density quantification

We investigated APNpI and PBS injected animals (5 animals or 15 spots per group) at day 10 post laser injury. We captured hematoxylin and eosin stained sections (3 sections per one laser spot) and close sections stained by IHC for endothelial marker Von Willebrand Factor. Vessels in the laser injured area were identified by morphological signs (oval shaped structures with lumen or blood cells inside) and presence of specific staining for Von Willebrand Factor. Laser injured areas were countered manually using the ImageJ program (National Institute of Health, Bethesda, MD). Number of vessels in this area was counted and number of vessels per 1 mm^2 was calculated.

2.10. Quantification of immunofluorescence in laser spots

Paraffin sections (5 animals or 15 spots per group) of IHC stained for VEGF, VEGF-R2 and endothelial marker isolectin IB4 were investigated using ZEISS LSM 510 laser confocal microscope. Composite images of differential interference contrast (DIC), red (endothelial

cells) and green (VEGF or VEGF-R2) were captured. Isolectin IB4 positive vessels and RPE cells were identified using DIC images and manually countered. Mean intensity of VEGF or VEGF-R2 positive signal was measured separately in 1) RPE cells, 2) isolectin IB4 positive vessels and 3) the rest of the choroid (in naïve animals) or subretinal tissue (in laser treated rats) using the ImageJ program (National Institute of Health, Bethesda, MD).

2.11. Quantification of PCNA ploliferative index

We used sections of APNpI and PBS treated animals (n=5 rats in each group) sacrificed at day 10 post laser injury. Sections were IHC stained for PCNA. Three sections from each laser injured area were captured, totally 15 laser spots sections per group were investigated. The number of PCNA positive nuclei (purple color) and total number of nuclei (purple and green color) in laser injured area were counted using ImageJ program (National Institute of Health, Bethesda, MD) and the percentage (%) of PCNA-positive nuclei was calculated.

2.12. RT-PCR analysis

Five animals from each group were sacrificed and RPE-choroids were harvested from the enucleated eyes. Total RNA was extracted from the tissue with RNeasy Mini Kit (QIAGEN, Valencia, CA). Equal amounts of the total RNA (0.1 μg) were used to detect the mRNA levels of β-actin, VEGF and VEGF-R2 by RT-PCR using the reagents from Applied Biosystems (Foster City, CA). Oligonucleotide primers were obtained from Integrated DNA Technologies (San Diego, CA). The negative controls consisted of omission of RNA or reverse transcriptase from the reaction mixture. PCR products were analyzed on a 1% agarose gel and were examined by using Quantity One (Bio-Rad, Hercules, CA). RT-PCR was conducted using the following primers: β-actin (F, 5’- GCG CTC GTC GTC GAC AAC GG -3’; R, 5’- GTG TGG TGC CAA ATC TTC TCC - 3’; VEGF (F, 5'- GCG GGC TGC TGC AAT GAT-3'; R, 5'-TCA CCG CCT TGG CTT GTC AC- 3'); VEGF-R2 (F, 5'- GCT TGC CTT ATG ATG CCA GCA AGT-3'; R, 5'- GGG CCA AGC CAA AGT CAC AGA TTT- 3'). Experiment was repeated three times with similar results.

2. 13. Real-time quantitative RT-PCR (RT-qPCR)

Naïve non treated animals and animals at day 10 post laser injury were sacrificed and RPE-choroid tissue harvested from the enucleated eyes. Total RNA was purified using the RNeasy mini kit (Qiagen, Valencia, CA), and cDNA was synthesized using the iScript cDNA synthesis kit (Bio-Rad, Hercules CA) with 0.5 μg of total RNA according to the manufacturer's recommendations. qPCR was performed with primers specific for rat APN, VEGFA, VEGF-R2 and β-actin using iQ SYBR Green Supermix in an iQ5 real-time PCR detection system (Bio-Rad, Hercules CA). The primers were designed and ordered from Integrated DNA Technologies (Coralville, IA). The primer sequences used were as follows: rat APN, 5′-CGG TAT CCC ATT GTG ACC AG-3′ (forward) and 5′- CGC TCC TG TTC CTC TTA ATC C-3′ (reverse); rat VEGF, 5′-CTC TTT TCT CTG CCT CCA TGA-3′ (forward) and 5′-CCA TTG AAA CCA CTA ATT CTG TCC-3′ (reverse); VEGF-R2 5′-GAG TAG CCA TGC ACC GAA T-3′ (forward) and 5′-CGG CTG TCC ATG AAA GTG AA-3′ (reverse);and rat β-actin, 5′-AAC CCT AAG GCC AAC CGT GAA A-3′ (forward) and 5′-AGG CAT ACA GGG ACA ACA CA-3′ (reverse). Pilot real-time RT-qPCR experiments were performed to determine the optimal condition for each primer. All real-time RT-qPCR experiments were performed in duplicate. The primer specificity of the amplification product was confirmed by melting curve analysis of the reaction products using SYBR Green as well as by visualization on ethidium bromide-stained agarose (1.5%) gels. The housekeeping gene β-actin was used as an internal control, and the gene-specific mRNA expression was normalized against β-actin expression. iQTM5 optical system software (Bio-Rad; version 2.0) was used to analyze real-time RT-qPCR data and derive threshold cycle (CT) values according to the manufacturer's instructions. The ΔΔCT method

was used to transform CT values into relative quantities with S.D. The same software was used to calculate the normalized expression of the gene of interest, using β-actin as reference gene, and the results were expressed as normalized fold expression.

2.14 Semi-quantitative Western blot analysis

Total protein was extracted from the pooled RPE-choroid tissue. The tissue was homogenized and solubilized in ice-cold PBS containing protease inhibitors and detergent NP-40. Electrophoresis was performed on 7.5% SDS-PAGE slab gel and the separated proteins were transferred to polyvinylidene difluoride (PVDF) membranes. The blots were blocked with 5% non-fat dry milk. Goat polyclonal anti-rat VEGFA antibody (R&D Systems, Minneapolis, MN) and rabbit polyclonal anti-VEGF receptor 2 antibody (Affinity Bioreagents, Golden, CO) was used as the primary antibodies and the blots were incubated overnight at +4°C. The control blots were reacted with equivalent concentration of isotype matched purified IgG. Blots were developed using the enhanced chemiluminescence Western blotting detection system “ECL + Plus” (Amersham Pharmacia Biotech, Arlington Heights, IL) according to manufacturer's recommendations. Quantification of VEGF, VEGF-R2 and β-actin was accomplished by analyzing the intensity of the bands using Quantity one 4.2.0 (Bio-Rad). Experiment was repeated three times with similar results.

2.15. Statistical analysis

Comparison between groups was performed with Statistica program (StatSoft, Tulsa, OK) using ANOVA/MANOVA analysis (post-hoc comparisons, Newman-Keuls test). Data presented as mean±SE. Significance was defined at $p<0.05$.

3. Results

3.1. Expression of adiponectin receptors and adiponectin in rat CNV

We investigated the expression of APN and its receptors in naïve and laser treated rat eyes at day 10 post laser injury using method of IHC. Adiponectin receptors R1 (AdipoR1) and R2 (AdipoR2) were found in RPE cells and choroidal vessels of naïve animals (fig. 1A, B) and in the CNV areas of laser treated rats (fig. 1E, F). Semiquantitative evaluation of IHC staining on paraffin sections showed that the expression of AdipoR1 was significantly increased at day 10 after laser treatment compared to naïve control (fig. 1I). We did not found difference of staining for AdipoR2 between experimental groups (fig. 1J). Positive staining for APN was localized in large and medium sized vessels of the naïve rat choroid (fig. 1C, D). At day 10 post laser injury intensity of APN staining in choroid vessels increased (fig. 1G, H) compared to naïve rats. Some APN positive new vessels were located in the subretinal tissue (fig. 1G). Real-time PCR analysis of RPE-choroid tissue detected increased expression of APN mRNA in the laser treated animals compared to the naïve animals (fig. 1K).

3.2. Colocalization of adipoR1 receptors and APNpI

We observed binding of APNpI-FITC to RPE-choroid tissue in vivo and to CECs in vitro. APNpI was colocalized with adipoR1 (fig. 2A, C, E). However, no background autofluorescence of the tissues and cells was observed (fig. 2B, D and F).

3.2. Effect of APNpI on size of CNV

In the present study we investigated effect of systemic administration of APNpI in rat model of CNV. PBS treated animals had well developed CNV complex and FITC-dextran perfused vessels occupied 25% of laser spot. After APNpI treatment size of CNV decreased 4 fold compared to control (fig. 3). To confirm anti-angiogenic effect of APNpI we investigated

serial paraffin sections of rat eyes stained with hematoxylin/eosin and endothelial marker vWF. APNpI treated animals at day 10 post laser injury had 40% smaller size of subretinal tissue and decreased density of vessels (2 fold) compared to the control (fig. 4).

3.3. Effect of APNpI on VEGF and VEGF-R2 expression

We found that APNpI administration decreased VEGF mRNA and protein levels in RPE-choroid tissue complex at day 10 post laser injury (fig. 5). IHC investigation of VEGF expression in naïve animals showed that RPE cells and choroidal vessels were major sources of VEGF in the RPE-choroid complex (51.3% and 47.3% of all VEGF in this tissue, respectively). All other choroidal structures contained only 1.4% of VEGF. Expression of VEGF increased in RPE cells (26%, G, J, L), choroidal vessels (50%, fig. 5 G, J, M) and subretinal tissue (26 fold, fig. 5 G, J, N) at day 10 post laser injury compared to naïve rats. APNpI administration significantly decreased VEGF in RPE cells and vessels and completely normalized it (fig. 5 H, K, M, N). Treatment with APNpI reduced (1.6 fold) level of VEGF in subretinal tissue compared to PBS treated group (fig. 5 H, K, N).

We determined that VEGF-R2 mRNA expression in RPE-choroid increased 2 fold at day 10 post laser injury compared to the naïve control (fig. 6 A, C). Administration of APNpI normalized VEGF-R2 level at day 10 after laser. IHC investigation showed that mean intensity of VEGF-R2 positive immunofluorescence was increased in RPE cells and in subretinal tissue (fig. 6 G, J, L, N) at day 10 post laser injury compared to the naïve control (fig. 6 F, I, L, N). Administration of APNpI decreased VEGF-R2 levels in subretinal tissue 4 fold at day 10 post laser injury and normalized it (fig. 6 H, K, N). Expression of VEGF-R2 in Isolectin IB4 positive vessels was the same at day 10 post laser injury in APNpI and PBS treated groups and was equal to the naïve control (fig. 6 F–K, M). In vitro study confirmed that APNpI has no effect on expression of VEGF-R2 mRNA in CECs (fig. 6 E).

3.4. Effect of APNpI on PCNA proliferative index

We investigated PCNA proliferative index in laser spots of PBS and APNpI treated animals using method of IHC. We found that at day 10 post laser injury APNpI treated rats had significantly (4 fold) decreased PCNA positive nuclei in laser spot (fig. 7).

4. Discussion

Adiponectin is produced mostly by adipose tissue and present in blood in high amount [20, 27–29]. Adipocyte derived APN represents basic level of the hormone necessary to perform its numerous functions [10, 27]. Local production of APN by non adipose tissues contributes to regulation of local processes like inflammation, regeneration and neovascularization [9, 10,15]. Adiponectin circulates in the blood in full length form, globular APN may originate from full form by proteolytic cleavage [30]. We designed APN peptide I from the globular domain of APN.

In this study we have shown that medium and large sized choroidal vessels expressed APN in naïve rats. Formation of CNV after laser injury was characterized by increased expression of APN in new formed vessels. The adiponectin receptors (AdipoR1 and AdipoR2) were found in rat choroid and RPE cells. But only AdipoR1 was up-regulated in RPE cells and new vessels of mature CNV. We found in the present study that both APN and its receptors expressed in endothelial cells of the choroid and cultured CECs. AdipoR1 expression was also found in human and bovine lines of endothelial cells [14]. AdipoR1 is receptor mostly for globular APN and AdipoR2 is for full-length APN [7, 27].

To determine effects of APN in CNV we investigated the role of APNpI in rat model of CNV in vivo and on CECs in culture. APNpI was accumulated in CNV and CECs and

colocalized with AdipoR1. We found that APNpI decreased the size and the number of newly formed choroidal vessels. APN may be important in the regulation of angiogenesis since increased levels of APN have anti-angiogenic effects [10]. Possible mechanisms of APN action may include anti-inflammatory action which involves regulation of pro-inflammatory cytokines and growth factors [7, 9, 13–18, 27].

VEGF and other growth factors promote development of CNV [3–5]. Reduction of VEGF is a key event in the treatment of AMD [4]. VEGF was found in the proliferating RPE cells, choroidal endothelial cells, inflammatory cells and subretinal tissue [31, 32] after induction of CNV. We investigated the expression of VEGF on day 10 post laser injury when the network of new vessels is formed. We found increased level of VEGF mRNA and protein in the RPE-choroid tissue complex of rats at day 10 post laser injury compared to naïve (non-lasered) animals. Under microscopic examination of IHC stained sections of naïve rats we found that the VEGF is expressed mostly in RPE and choroidal vessels. At day 10 post laser injury we found that the VEGF in RPE and choroidal vessels was increased however, the most impressive changes were observed in subretinal tissues compared to the choroid of naïve animals. APNpI treatment normalized expression of VEGF in RPE cells and choroidal vessels and reduced amount of VEGF in subretinal tissue.

VEGF is involved in cellular proliferation mostly mediated through its receptor VEGF-R2 [33]. We tested levels of VEGF-R2 and found that APNpI did not change expression of VEGF-R2 in choroidal vessels and CECs in culture. However, VEGF-R2 in subretinal tissue was significantly reduced. This observation shows that reduction of VEGF expression by APNpI did not induce over-expression of its receptors but reduced VEGF-R2 expression in subretinal tissues.

Previous studies have shown that the full length APN inhibited proliferation of endothelial cells *in vitro* and *in vivo* [11, 14, 27]. APN also inhibited proliferation of other type of cells like vascular smooth muscle cells [13, 34], keratinocytes [35], cancer cells [36–38].

Here we propose mechanism of anti-angiogenic action of APN in the rat model of CNV. APNpI accumulates on AdipoR1-positive RPE cells and choroidal vessels, reduces production and secretion of VEGF, which leads to low PCNA expression and reduced cell proliferation thus decreasing formation of new vessels. Our results show that the APNpI inhibited formation of new choroidal vessels and reduced the neovascular size and density. Thus in future, the peptide (APNpI) may be helpful in the treatment of wet type of AMD in humans.

Acknowledgments

This study was supported in part by NIH grants EY 014623 & EY 016205, Pat & Willard Walker Eye Research Center, Jones Eye Institute and Arkansas Master Tobacco Settlement and Arkansas Biosciences Institute, University of Arkansas for Medical Sciences, Little Rock, AR.

References

1. Friedman DS, O'Colmain BJ, Muñoz B, Tomany SC, McCarty C, de Jong PT, Nemesure B, Mitchell P, Kempen J. Eye Diseases Prevalence Research Group. Prevalence of age-related macular degeneration in the United States. Arch. Ophthalmol. 2004; 122:564–572. [PubMed: 15078675]
2. Coleman HR, Chan CC, Ferris FL 3rd, Chew EY. Age-related macular degeneration. Lancet. 2008; 372:1835–1845. [PubMed: 19027484]
3. Gehrs KM, Anderson DH, Johnson LV, Hageman GS. Age-related macular degeneration - emerging pathogenetic and therapeutic concepts. Ann. Med. 2006; 38:450–471. [PubMed: 17101537]

4. Ciulla TA, Rosenfeld PJ. Antivascular endothelial growth factor therapy for neovascular age-related macular degeneration. Curr. Opin. Ophthalmol. 2009; 2:158–165. [PubMed: 19417570]
5. Campochiaro PA. Retinal and choroidal neovascularization. J. Cell. Physiol. 2000; 184:301–310. [PubMed: 10911360]
6. Day S, Acquah K, Mruthyunjaya P, Grossman DS, Lee PP, Sloan FA. Ocular complications after anti-vascular endothelial growth factor therapy in Medicare patients with age-related macular degeneration. Am. J. Ophthalmol. 2011; 152:266–272. [PubMed: 21664593]
7. Kadowaki T, Yamauchi T. Adiponectin and adiponectin receptors. Endocr. Rev. 2005; 26:439–451. [PubMed: 15897298]
8. Kadowaki T, Yamauchi T, Kubota N. The physiological and pathophysiological role of adiponectin and adiponectin receptors in the peripheral tissues and CNS. FEBS Lett. 2008; 582:74–80. [PubMed: 18054335]
9. Sun Y, Xun K, Wang C, Zhao H, Bi H, Chen X, Wang Y. Adiponectin, an unlocking adipocytokine. Cardiovasc. Ther. 2009; 27:59–75. [PubMed: 19207481]
10. Zhu W, Cheng KK, Vanhoutte PM, Lam KS, Xu A. Vascular effects of adiponectin: molecular mechanisms and potential therapeutic intervention. Clin. Sci. (Lond). 2008; 114:361–374. [PubMed: 18230060]
11. Brakenhielm E, Veitonmaki N, Cao R, Kihara S, Matsuzawa Y, Zhivotovsky B, Funahashi T, Cao Y. Adiponectin-induced antiangiogenesis and antitumor activity involve caspase-mediated endothelial cell apoptosis. Proc. Natl. Acad. Sci. U S A. 2004; 101:2476–2481. [PubMed: 14983034]
12. Ouchi N, Kobayashi H, Kihara S, Kumada M, Sato K, Inoue T, Funahashi T, Walsh K. Adiponectin stimulates angiogenesis by promoting cross-talk between AMP-activated protein kinase and Akt signaling in endothelial cells. J. Biol. Chem. 2004; 279:1304–1309. [PubMed: 14557259]
13. Wang Y, Lam KS, Xu JY, Lu G, Xu LY, Cooper GJ, Xu A. Adiponectin inhibits cell proliferation by interacting with several growth factors in an oligomerization-dependent manner. J. Biol. Chem. 2005; 280:18341–18347. [PubMed: 15734737]
14. Motoshima H, Wu X, Mahadev K, Goldstein BJ. Adiponectin suppresses proliferation and superoxide generation and enhances eNOS activity in endothelial cells treated with oxidized LDL. Biochem. Biophys. Res. Commun. 2004; 315:264–271. [PubMed: 14766203]
15. Bora PS, Kaliappan S, Lyzogubov VV, Tytarenko RG, Thotakura S, Viswanathan T, Bora NS. Expression of adiponectin in choroidal tissue and inhibition of laser induced choroidal neovascularization by adiponectin. FEBS Lett. 2007; 581:1977–1982. [PubMed: 17466298]
16. Lyzogubov VV, Tytarenko RG, Thotakura S, Viswanathan T, Bora NS, Bora PS. Inhibition of new vessel growth in mouse model of laser-induced choroidal neovascularization by adiponectin peptide II. Cell Biol. Int. 2009; 33:765–771. [PubMed: 19422927]
17. Krenning G, Moonen JR, Harmsen MC. Pleiotropism of adiponectin: inflammation, neovascularization, and fibrosis. Circ. Res. 2009; 104:1029–1031. [PubMed: 19423859]
18. Higuchi A, Ohashi K, Kihara S, Walsh K, Ouchi N. Adiponectin suppresses pathological microvessel formation in retina through modulation of tumor necrosis factor-alpha expression. Circ. Res. 2009; 104:1058–1065. [PubMed: 19342600]
19. Mahadev K, Wu X, Donnelly S, Ouedraogo R, Eckhart AD, Goldstein BJ. Adiponectin inhibits vascular endothelial growth factor-induced migration of human coronary artery endothelial cells. Cardiovasc. Res. 2008; 78:376–384. [PubMed: 18267956]
20. Scherer PE, Williams S, Fogliano M, Baldini G, Lodish HF. A novel serum protein similar to C1q, produced exclusively in adipocytes. Biol. Chem. 1995; 270:26746–26749.
21. Zubilewicz A, Hecquet C, Jeanny J, Soubrane G, Courtois Y, Mascarelli F. Proliferation of CECs requires dual signaling through both MAPK/ERK and PI 3-K/Akt pathways. Invest. Ophthalmol. Vis. Sci. 2001; 42:488–496. [PubMed: 11157888]
22. Bora PS, Hu Z, Tezel TH, Sohn JH, Kang SG, Cruz JM, Bora NS, Garen A, Kaplan HJ. Immunotherapy for choroidal neovascularization in a laser-induced mouse model simulating exudative (wet) macular degeneration. Proc. Natl. Acad. Sci. U S A. 2003; 100:2679–2684. [PubMed: 12589025]

23. Bora PS, Sohn JH, Cruz JM, Jha P, Nishihori H, Wang Y, Kaliappan S, Kaplan HJ, Bora NS. Role of complement and complement membrane attack complex in laser-induced choroidal neovascularization. J. Immunol. 2005; 174:491–497. [PubMed: 15611275]
24. Bora NS, Kaliappan S, Jha P, Xu Q, Sohn JH, Dhaulakhandi DB, Bora PS. Complement activation via alternative pathway is critical in the development of laser-induced choroidal neovascularization: role of factor B and factor H. J. Immunol. 2006; 177:1872–1878. [PubMed: 16849499]
25. Kaliappan S, Jha P, Lyzogubov VV, Tytarenko RG, Bora NS, Bora PS. Alcohol and nicotine consumption exacerbates choroidal neovascularization by modulating the regulation of complement system. FEBS Lett. 2008; 582:3451–3458. [PubMed: 18789935]
26. Edelman JL, Castro MR. Quantitative image analysis of laser-induced choroidal neovascularization in rat. Exp. Eye Res. 2000; 71:523–533. [PubMed: 11040088]
27. Goldstein BJ, Scalia R. Adiponectin: A novel adipokine linking adipocytes and vascular function. J. Clin. Endocrinol. Metab. 2004; 89:2563–2568. [PubMed: 15181024]
28. Shibata R, Ouchi N, Murohara T. Adiponectin and cardiovascular disease. Circ. J. 2009; 73:608–614. [PubMed: 19261992]
29. Arita Y, Kihara S, Ouchi N, Takahashi M, Maeda K, Miyagawa J, Hotta K, Shimomura I, Nakamura T, Miyaoka K, Kuriyama H, Nishida M, Yamashita S, Okubo K, Matsubara K, Muraguchi M, Ohmoto Y, Funahashi T, Matsuzawa Y. Paradoxical decrease of an adipose-specific protein, adiponectin, in obesity. Biochem. Biophys. Res. Commun. 1999; 257:79–83. [PubMed: 10092513]
30. Waki H, Yamauchi T, Kamon J, Kita S, Ito Y, Hada Y, Uchida S, Tsuchida A, Takekawa S, Kadowaki T. Generation of globular fragment of adiponectin by leukocyte elastase secreted by monocytic cell line THP-1. Endocrinology. 2005; 146:790–796. [PubMed: 15528304]
31. Yi X, Ogata N, Komada M, Yamamoto C, Takahashi K, Omori K, Uyama M. Vascular endothelial growth factor expression in choroidal neovascularization in rats. Graefes. Arch. Clin. Exp. Ophthalmol. 1997; 235:313–319. [PubMed: 9176680]
32. Shen WY, Yu MJ, Barry CJ, Constable IJ, Rakoczy PE. Expression of cell adhesion molecules and vascular endothelial growth factor in experimental choroidal neovascularisation in the rat. Br. J. Ophthalmol. 1998; 82:1063–1071. [PubMed: 9893599]
33. Matsumoto T, Mugishima H. Signal transduction via vascular endothelial growth factor (VEGF) receptors and their roles in atherogenesis. J. Atheroscler. Thromb. 2006; 13:130–135. [PubMed: 16835467]
34. Matsuda M, Shimomura I, Sata M, Arita Y, Nishida M, Maeda N, Kumada M, Okamoto Y, Nagaretani H, Nishizawa H, Kishida K, Komuro R, Ouchi N, Kihara S, Nagai R, Funahashi T, Matsuzawa Y. Role of adiponectin in preventing vascular stenosis. The missing link of adipo-vascular axis. J. Biol. Chem. 2002; 277:37487–37491. [PubMed: 12138120]
35. Kawai K, Kageyama A, Tsumano T, Nishimoto S, Fukuda K, Yokoyama S, Oguma T, Fujita K, Yoshimoto S, Yanai A, Kakibuchi M. Effects of adiponectin on growth and differentiation of human keratinocytes - implication of impaired wound healing in diabetes. Biochem. Biophys. Res. Commun. 2008; 374:269–273. [PubMed: 18639522]
36. Ogunwobi OO, Beales IL. Globular adiponectin, acting via adiponectin receptor-1, inhibits leptin-stimulated esophageal adenocarcinoma cell proliferation. Mol. Cell. Endocrinol. 2008; 285:43–50. [PubMed: 18313838]
37. Nakayama S, Miyoshi Y, Ishihara H, Noguchi S. Growth-inhibitory effect of adiponectin via adiponectin receptor 1 on human breast cancer cells through inhibition of S-phase entry without inducing apoptosis. Breast Cancer Res. Treat. 2008; 112:405–410. [PubMed: 18163210]
38. Ishikawa M, Kitayama J, Yamauchi T, Kadowaki T, Maki T, Miyato H, Yamashita H, Nagawa H. Adiponectin inhibits the growth and peritoneal metastasis of gastric cancer through its specific membrane receptors AdipoR1 and AdipoR2. Cancer Sci. 2007; 98:1120–1127. [PubMed: 17459059]

Highlights

Adiponectin peptide I (APNpI) inhibited area of CNV by 4 fold.

The expression of VEGF and VEGF-R2 was decreased after APNpI treatment.

Proliferative index (PCNA) was 5 fold less in laser spots of APNpI treated rats.

APNpI inhibited formation of new vessels in rat model of CNV.

APNpI may have therapeutic use for AMD treatment.

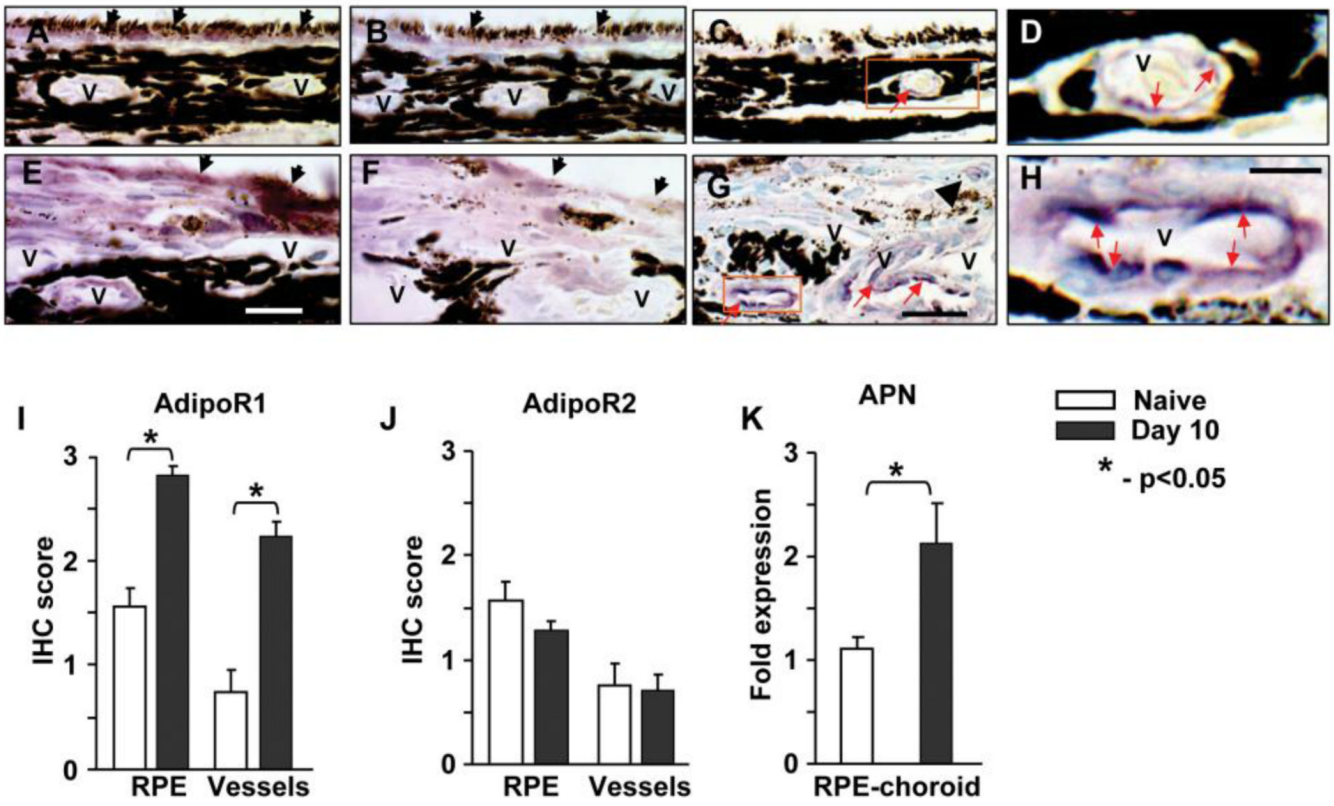

Figure 1.

Localization and expression of adiponectin receptors and adiponectin in rat CNV. Eyes from naïve rats and laser treated animals were sacrificed at day 10 post laser injury and IHC stained for adiponectin. Positive staining is purple (red arrow), nuclei are green. Representative images of IHC staining for AdipoR1 (A, E) and AdipoR2 (B, F). RPE cells (black arrow), choroidal vessels (v) and other cells were positive (purple color) for adiponectin receptors. Semiquantitative scoring of IHC for AdipoR1 (I) and AdipoR2 (J) in RPE cells and choroidal vessels. Expression of AdipoR1 was increased in RPE cells and choroidal vessels at day 10 after laser compared to naïve control. Adiponectin was detected in endothelial cells of choroidal vessels (v) of naïve animals (C, D) and in laser spots (G, H). Expression of APN in laser injured and naïve control RPE-choroid tissue was investigated by real-time PCR. Significant increase of APN mRNA was found in RPE-choroid with laser induced CNV compared to naive control (K). Bar = 25 μm for images C and G; bar = 7 μm for images D and H. Images D and H are the enlargement of area shown in rectangle on images C and G, respectively. Bar for images A, B, E and F is 20 μm.

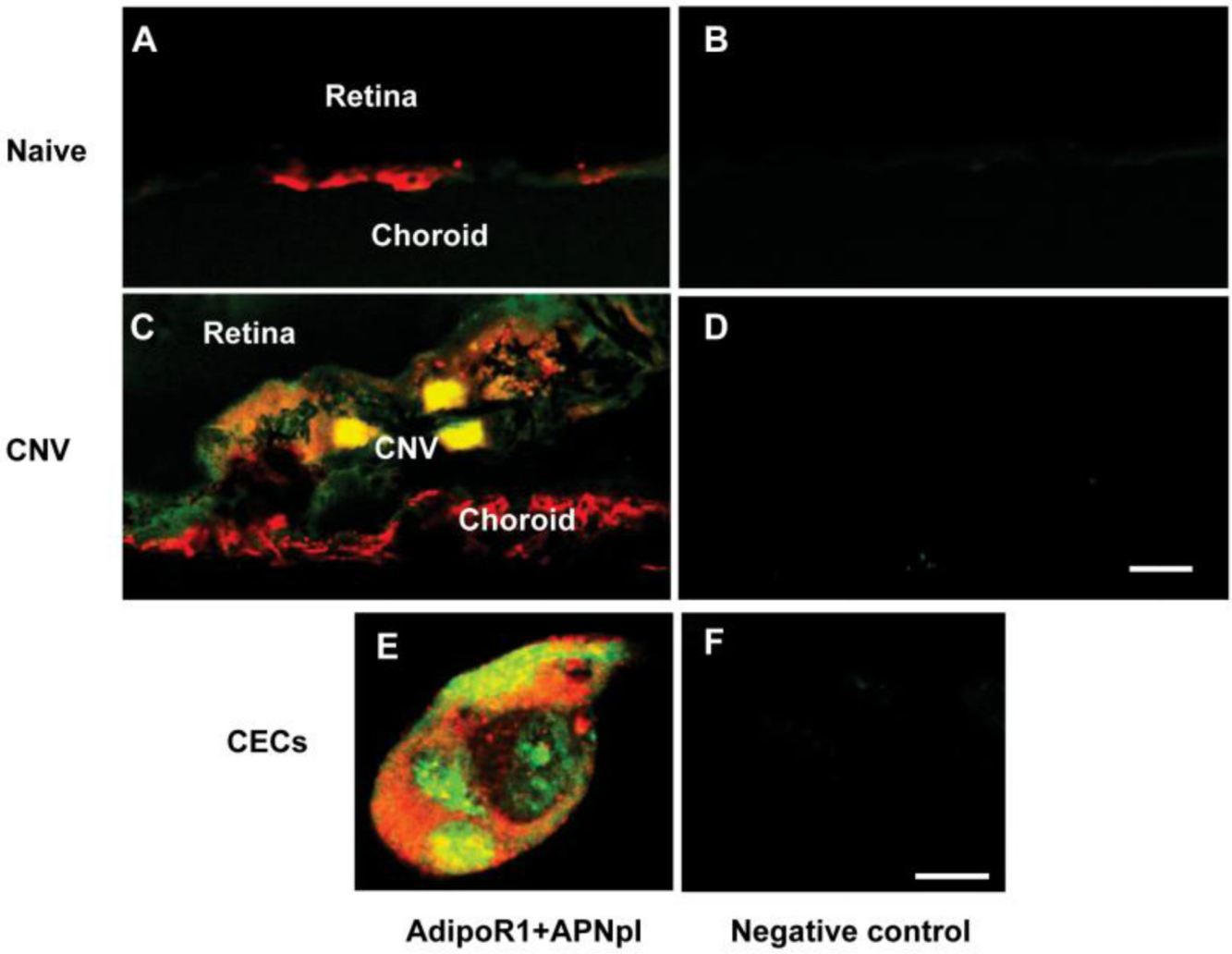

Figure 2.

Binding of APNpI to AdipoR1 positive cells. Laser confocal microscopic images of cryosections of naïve control (A, B), CNV on day 7 post laser injury (C, D) and CECs in culture (E, F). Yellow color represents colocalization of APNpI-FITC (green color) and AdipoR1 (red color). Accumulation of APNpI was found predominantly on cells with adipoR1 expression. There was very low autofluorescence of the tissues (B, D, F). Bar for A–D is 10 μm and for E and F is 10 μm.

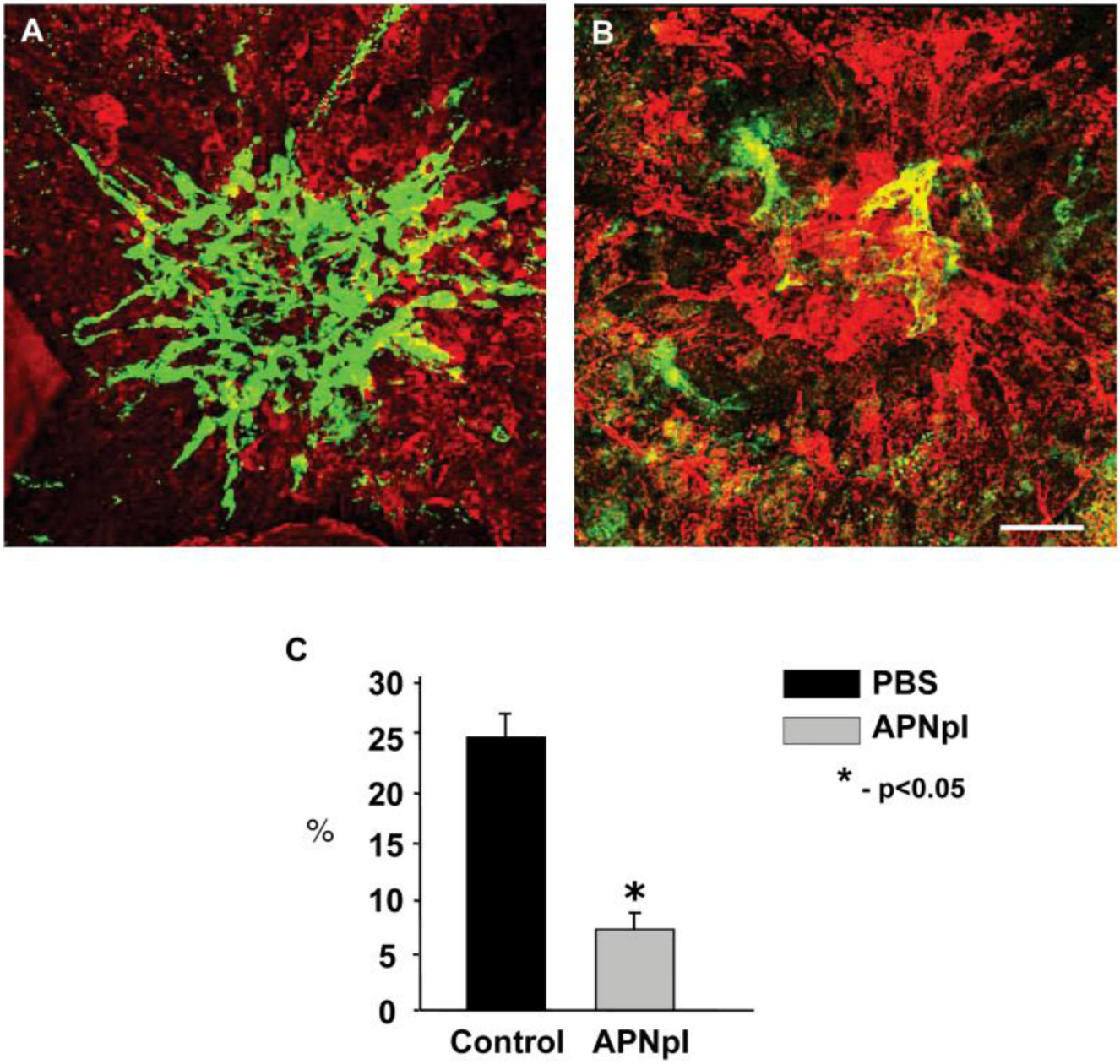

Figure 3.

Effect of APNpI on laser-induced CNV. (A, B) Laser confocal microscopic images of flat mounted RPE-choroid-sclera at day 10 post laser injury. Green color shows FITC-dextran perfused vessels and red color is IHC staining for elastin. There was significant decrease of CNV size after treatment with APNpI compared to the control (C). Bar for all images is 40 μm.

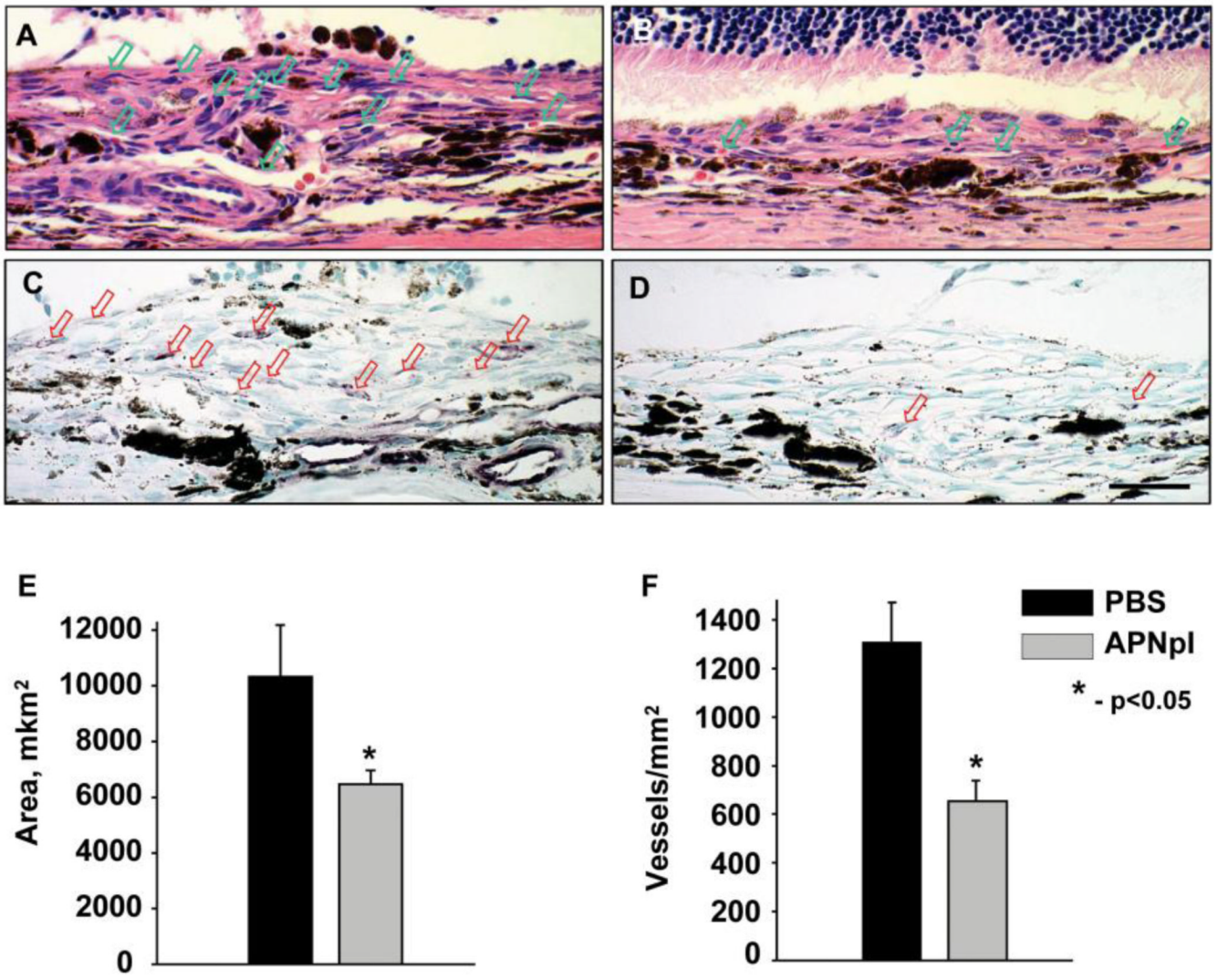

Figure 4.

Histological investigation of laser spot area of PBS (A, C) and APNpI (B, D) treated animals. Representative images of paraffin section stained with hematoxylin and eosin (A, B) and IHC for Von Willebrand Factor endothelial marker (C, D). Vessels marked with arrow. We determined significant decrease of area of subretinal tissue (E) and vessel density (F) in laser spot of APNpI treated rats compared to PBS treated animals. Bar for all images is 20 μm.

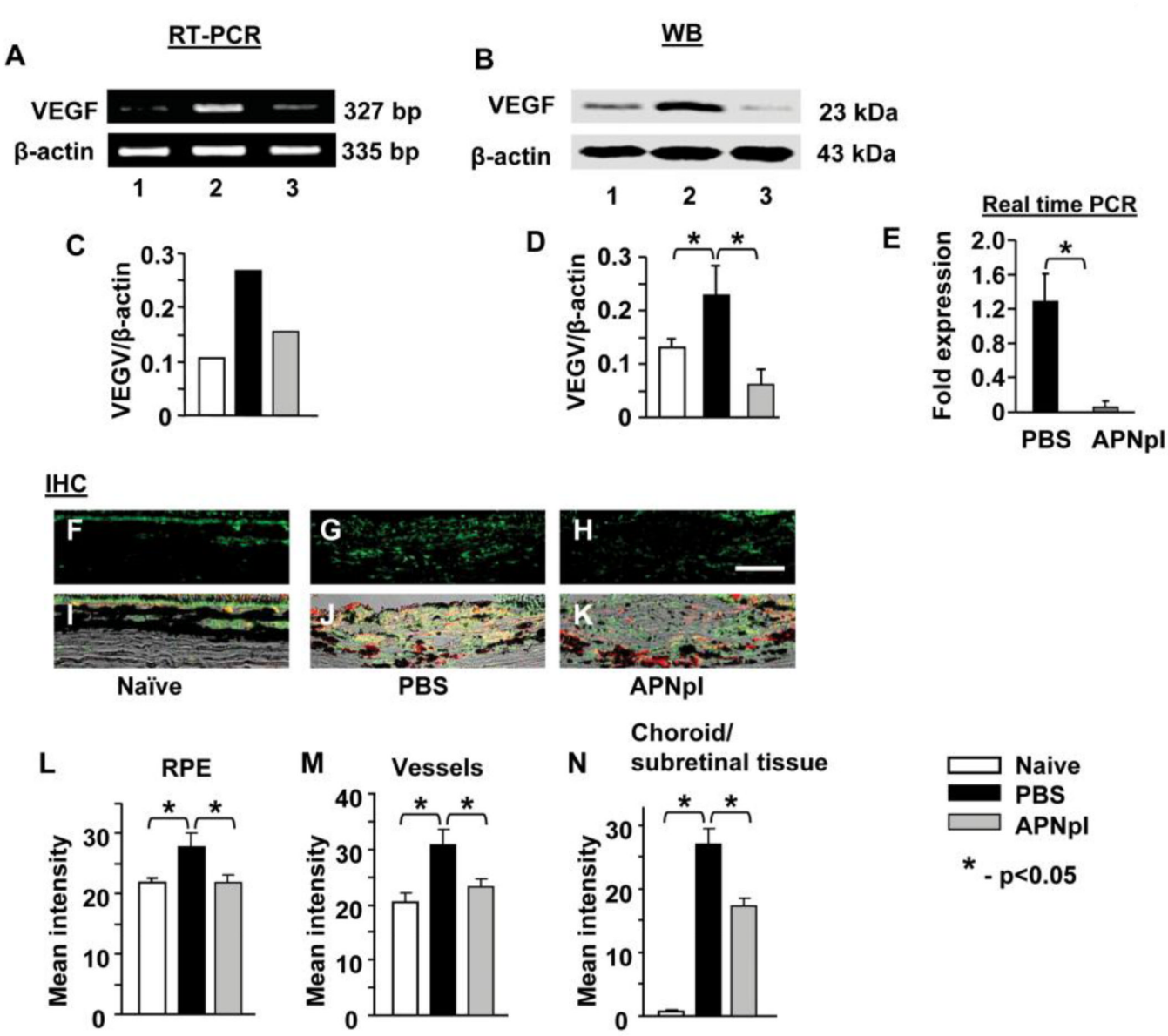

Figure 5.

Effect of APNpI on VEGF expression. (A) RT-PCR products for VEGF in RPE-choroid-sclera of naïve, APNpI and PBS treated rats (n=6 rats in each group) at 10 post laser injury. APNpI decreased VEGF mRNA (327 bp) expression. A strong band for β-actin (335 bp) indicates equal amounts of RNA in each lane. (C) Densitometric analysis of PCR products. Western blot analysis of RPE-choroid tissue shows that laser treatment increases expression of VEGFA (23 kDa) in RPE-choroid compared to naïve control (B, D). Real-time PCR analysis of VEGFA mRNA expression in choroidal endothelial cells showed significant down regulation of VEGFA after APNpI (80 μg/mL) treatment (E). (F–H) Representative images of IHC staining for VEGF (green color). (I–K) Merged DIC (black and white), VEGF (green) and Isolectin IB4 (red) images helps recognize RPE cells (pigmented cells in upper part of each image) and vessels (non pigmented oval shaped structures, positively marked with Isolectin IB4 in red color) and laser injured area. Quantification of mean intensity of fluorescence in RPE (L), choroidal vessels (M) and the rest of the choroid or

subretinal tissue (N) was done. VEGF expression significantly increased in all investigated structures at day 10 post laser injury (L, M, N). APNpI administration decreased expression of VEGF in RPE cells, vessels and laser injured area compared to PBS treated group. Bar for all images is 25 μm.

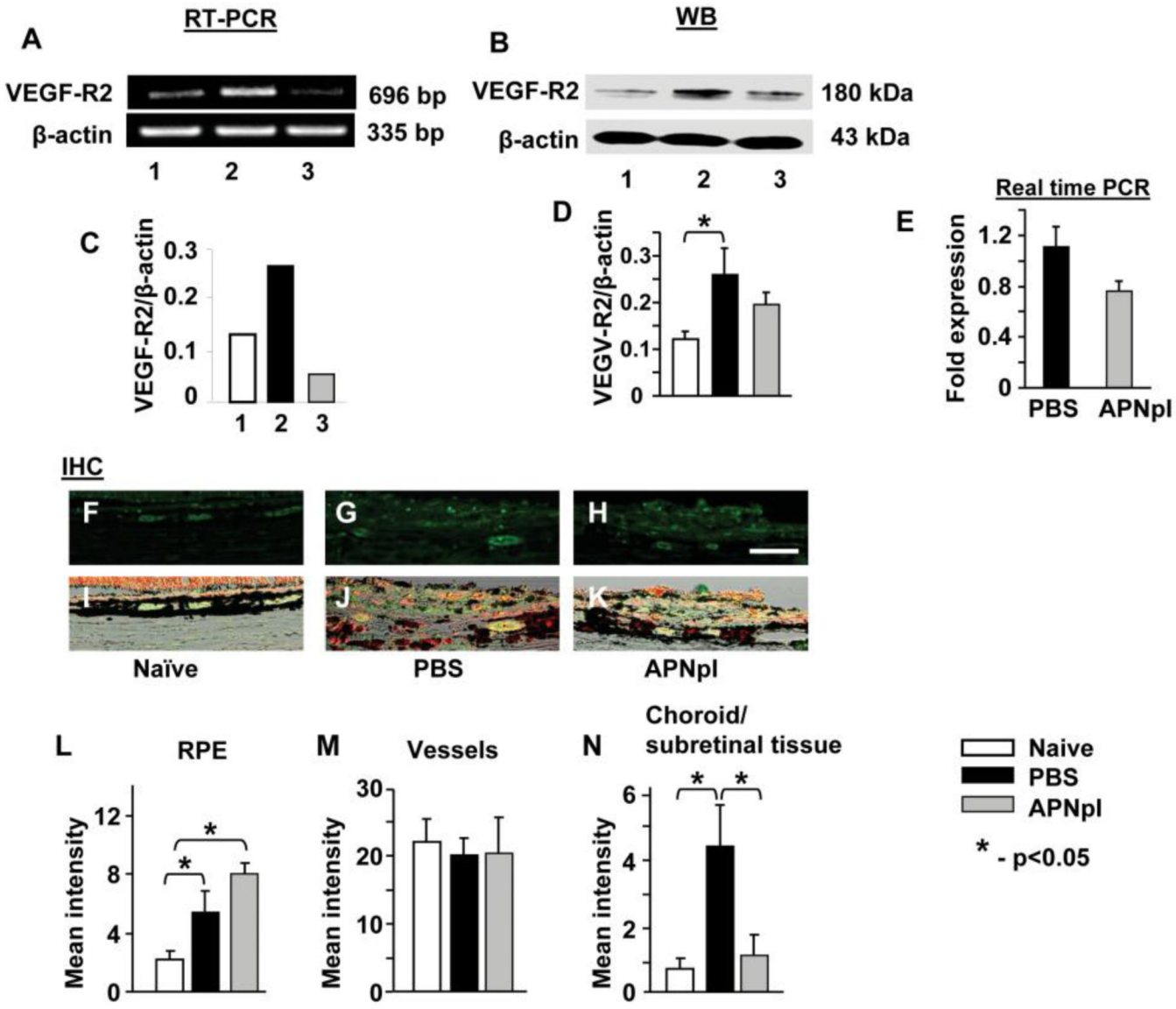

Figure 6.

Effect of APNpI on VEGF-R2 expression. (A) Ethidium bromide stained gel showing VEGF-R2 mRNA in RPE-choroid of naïve, APNpI and PBS treated rats at day 10 post laser injury. APNpI decreased VEGF-R2 mRNA (696 bp) at day 10 after laser treatment. (C) Densitometric analysis of PCR products. Western blot analysis of RPE-choroid tissue shows that laser treatment increases expression of VEGF-R2 (180 kDa) in RPE-choroid compared to naïve control (B, D). Real-time PCR analysis of VEGF-R2 mRNA expression in choroidal endothelial cells showed no significant changes of VEGF-R2 expression after APNpI (80 μg/mL) treatment (E). (F–H) Representative images of laser confocal microscopy of IHC staining for VEGF-R2 (green color) and (I–K) merged DIC (black and white), VEGF (green color) and Isolectin IB4 (red color) images. Quantification of mean intensity of immunofluorescence in RPE (L), choroidal vessels (M) and choroid or subretinal tissue (excluding vessels) (N). At day 10 post laser injury expression of VEGF-R2 increased in RPE cells and subretinal tissue compared to naïve control. APNpI administration decreased expression of VEGF-R2 in subretinal tissue compared to PBS treated groups. Bar for all images is 25 μm.

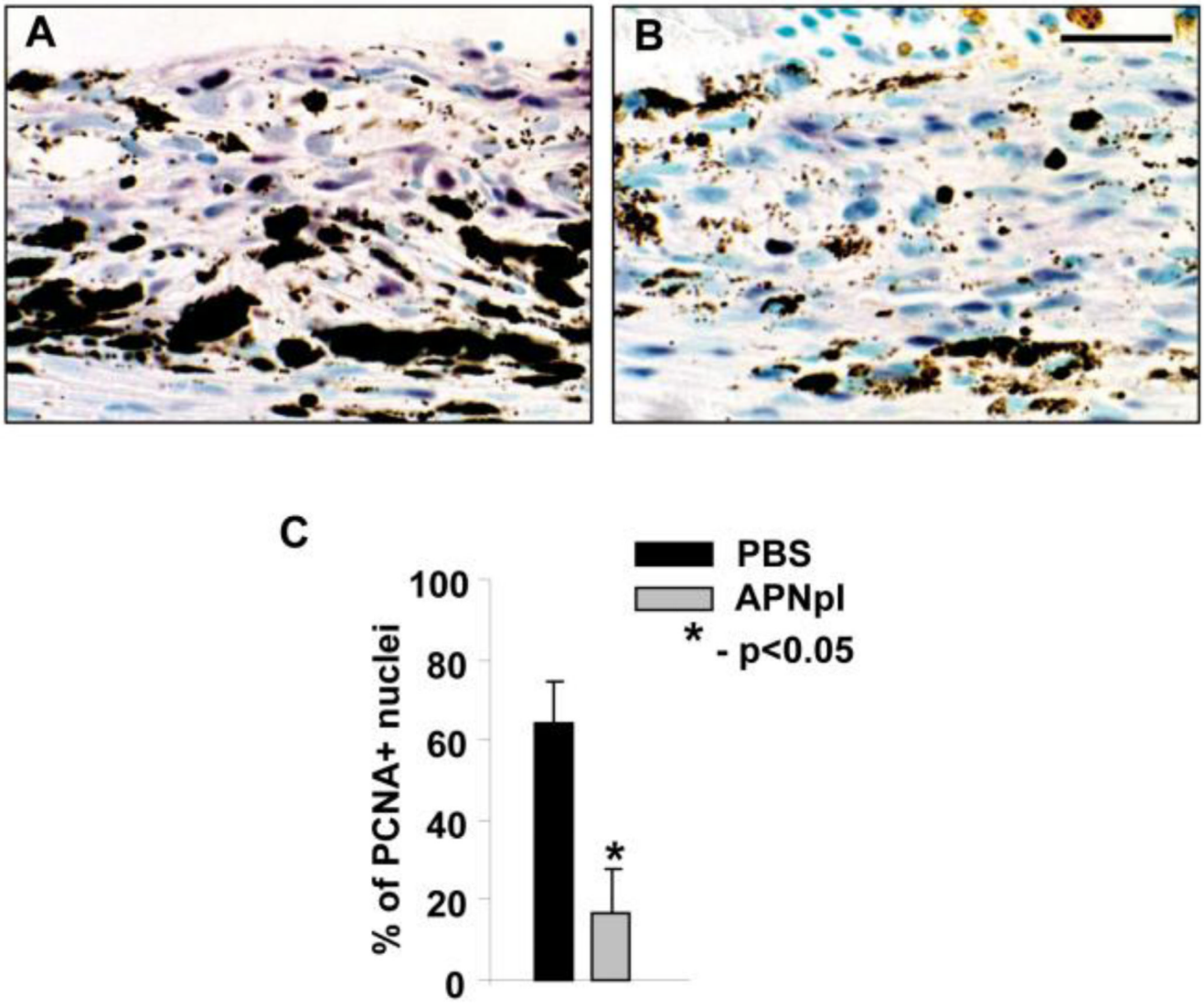

Figure 7.

APNpI influence on PCNA proliferative index in laser injured area. Representative images of paraffin sections stained by IHC method for PCNA from PBS (A) and APNpI (B) treated animals. PCNA positive nuclei are purple. Sections were counterstained with Methyl green. (C) A graph showing significant decrease of percentage of PCNA positive nuclei in APNpI treated group compared to PBS injected control. Bar for all images is 25 μm.